LOW THRUST AUGMENTED SPACECRAFT FORMATION-FLYING

Callum S Arnot [(1)], **Colin R McInnes** [(2)]

[(1)]*Department of Mechanical and Aerospace Engineering, University of Strathclyde, James Weir Building, Glasgow, G1 1XQ, +44 (0)141 330 8762, callum.arnot@strath.ac.uk*

[(2)]*School of Engineering, James Watt Building, University of Glasgow, Glasgow, G12 8QQ, +44 (0)141 330 8511, colin.mcinnes@glasgow.ac.uk*

Abstract: *Ballistic spacecraft formation-flying with zero thrust has great utility, but it is limited to a comparatively small set of relative trajectories. However, through the application of continuous low thrust, rich new families of formation-flying trajectories can be accessed. This new and novel problem provides a wide range of potentially useful alternatives to natural ballistic formation-flying. In this paper, the standard Clohessy-Wiltshire approximation of relative spacecraft motion is used to investigate the motion of a chase spacecraft about a target spacecraft which is in a circular Earth orbit. Families of non-Keplerian relative motion are systematically explored, generating analytical representations of the relative motion trajectories and the required thrust commands for both simple static formations and more complex new forced relative orbits. It is found that the impulse, and therefore propellant, required for maintenance of such relative orbits is small, and so the concept of low thrust augmented formation-flying is deliverable in the near term with existing thruster technology.*

Keywords: *Spacecraft Formation-Flying, Non-Keplerian Orbits, Rotating Reference Frame, Low Thrust Propulsion, Continuous Thrust.*

1. Introduction

A useful definition of spacecraft formation flying, given by the NASA Goddard Space Flight Center (GSFC) [1], is that it is "the tracking or maintenance of a desired relative separation, orientation, or position between or among spacecraft". An early extension of the concept was a proposed space-based infrared interferometer making use of several separate orbital telescopes, investigated by Sholomitsky, Prilutsky, and Rodin [2], and then similarly by Labeyrie [3]. Over the following decades, the conceptual value of such multi-spacecraft missions was explored, and in the late 1990s substantial interest developed for spacecraft formation-flying. The potential applications for spacecraft formation-flying have, in recent years, diversified greatly. Several such missions are in development or have flown; for example the ESA Project for On-Board Autonomy (PROBA-3) solar coronagraphy demonstrator [4], the Evolved Laser Interferometer Space Antenna (eLISA) [5], and several on-orbit inspection concepts such as the AeroAstro Escort [6].

The applications of Earth-orbiting spacecraft formations, in particular, are manifold: hyperspectral sensing, fractionated spacecraft, and multi-unit antenna arrays are examples of conceptual and planned Earth-orbiting missions [7, 8]. Most missions assume the use of chemical propulsion for relative motion control, however the low specific impulse of conventional thrusters imposes

limitations on the capabilities of the spacecraft formation. Most notably, the spacecraft will follow unforced ballistic trajectories for the majority of the mission [9]. Coulomb spacecraft formations (tethered and free-flying) have also been analysed by several authors as a means of propellantless control (e.g. [10, 11]).

It is therefore proposed that continuous low thrust, such as that provided by solar electric propulsion, could widen the scope of spacecraft formation-flying. Since the thrust magnitudes required for formation-keeping are generally small, several concepts for efficient electrostatic micro-thrusters would be suitable for this purpose (e.g. [12, 13]).

The use of continuous low thrust to counteract a component of gravity was apparently first suggested by Dusek, who proposed that artificial equilibria could be created in the vicinity of 3-body libration points [14]. The related concept of displacing the plane of a two-body orbit by using out-of-plane thrust was later explored by several authors, notably Austin et al., Nock, Yashko and Hastings, and McInnes [15, 16, 19], which are generally termed non-Keplerian orbits (NKOs) since the plane of the orbit does not contain the two-body centre of mass. A concept for creating displaced non-Keplerian geostationary orbits in which the continuous thrust is provided by a solar sail was considered by Baig and McInnes and Heiligers [17, 18], and numerous papers have established the conditions for the existence, stability, and controllability of such orbits [19-25]. In addition to continuous electric thrust and solar radiation pressure, the use of impulsive thrust has been considered as a means to maintain displaced NKOs. A comprehensive survey of non-Keplerian orbits and their potential applications has been provided by McKay et al. [26].

In this paper, rich new families of relative trajectories are generated by the addition of continuous low thrust, for the purposes of formation-flying. This new and novel problem provides a wide range of potentially useful alternatives to ballistic formation-flying trajectories. Using the Clohessy-Wiltshire approximation of motion in a rotating frame for a target and chase spacecraft formation in a circular Earth orbit, the relative motion of the spacecraft under low thrust is investigated. Families of non-Keplerian relative motion are systematically explored, generating analytical representations of the relative trajectories and the required thrust commands for both simple static formations and more complex new forced relative orbits.

The first such new class of forced relative orbits to be explored in this paper is a forced circular relative orbit which uses multi-axis thrust to permit circular relative orbits around the target spacecraft. The second class to be explored uses thrust in the out-of-plane direction to generate forced oscillatory motion, whose period is modifiable since the out-of-plane motion is decoupled from the in-plane motion. Once these orbit classes are established, they find combined application in a Sun vector tracking orbit, where the chase spacecraft tracks the Sun vector about the target spacecraft, since this type of relative orbit requires the chase spacecraft's in-plane and out-of-plane motion to have periods of one solar day and one year, respectively. Finally, this paper presents a simple and novel approach for patching between Keplerian and non-Keplerian orbits in the rotating frame, in particular between oppositely displaced non-Keplerian orbits, using both propellantless ballistic manoeuvres and low thrust manoeuvres.

2. Formation Flying in the Rotating Frame

Considering a target spacecraft which is in a circular reference orbit about a point-mass central body, the relative motion of a chase spacecraft with respect to the target spacecraft can be described by the linear Clohessy-Wiltshire equations [27]. In a frame of reference rotating with the target

spacecraft, the *x*-axis is along the radius vector to the target spacecraft, the *z*-axis is along the orbital angular momentum vector of the target spacecraft, and the *y*-axis completes the right-handed system by pointing in the direction of the target spacecraft's motion about the central body in the inertial reference frame, as shown in Figure 1.

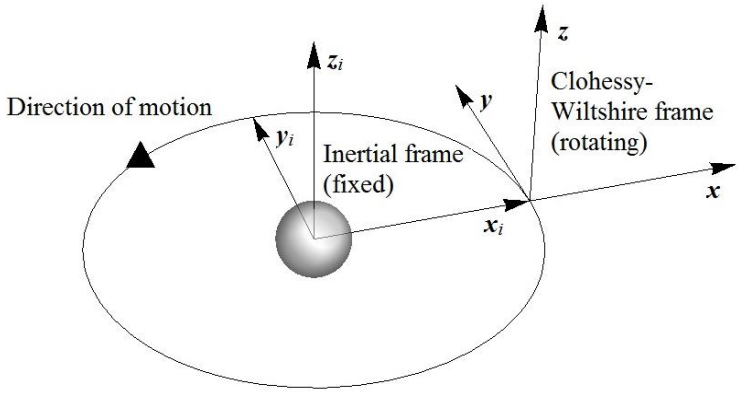

Figure 1. Clohessy-Wiltshire frame of reference.

Herein, motion along the *y*-axis is referred to as 'along-track'; motion along the positive and negative *z*-axis is referred to as 'out-of-plane', and motion along the *x*-axis is referred to as 'radial' motion. Using standard methods, the Clohessy-Wiltshire equations, modified by the addition of thrust terms, are found to be

$$\ddot{x} = 3n^2x + 2n\dot{y} + a_x \tag{1a}$$

$$\ddot{y} = -2n\dot{x} + a_y \tag{1b}$$

$$\ddot{z} = -n^2z + a_z \tag{1c}$$

where a_x, a_y and a_z are the continuous thrust-induced acceleration components in the *x*-, *y*-, and *z*-directions, respectively. When $a_x = a_y = a_z = 0$ the equations of motion in Eq. (1a-c) have the well-known closed-form solutions (for initial conditions x_0, $\dot{x}_0$, y_0, $\dot{y}_0$, z_0, $\dot{z}_0$ for position and velocity in the *x*-, *y*-, and *z*-axes respectively)

$$x(t) = \frac{\dot{x}_0}{n}\sin(nt) - \left(3x_0 + \frac{2\dot{y}_0}{n}\right)\cos(nt) + \left(4x_0 + \frac{2\dot{y}_0}{n}\right) \tag{2a}$$

$$y(t) = \frac{2\dot{x}_0}{n}\cos(nt) + \left(6x_0 + \frac{4\dot{y}_0}{n}\right)\sin(nt) - (6nx_0 + 3\dot{y}_0)t - \frac{2\dot{x}_0}{n} + y_0 \tag{2b}$$

$$z(t) = z_0\cos nt + \frac{\dot{z}_0}{n}\sin nt \tag{2c}$$

at time t, where the angular velocity of the rotating frame is given by

$$n = \sqrt{\frac{\mu}{R^3}} \tag{3}$$

where μ is the gravitational parameter and R is the radius of the target spacecraft's orbit about the central body in the inertial reference frame.

To maintain formation-flight between the target spacecraft and chase spacecraft, there must be zero secular variation in chase spacecraft relative position. In general, this means that there should be no secular term for the along-track (*y*-direction) motion. This does not, however, limit the pair of spacecraft to formations which are static along the *y*-axis: rather, periodic *y*-motion is made possible by correctly selecting initial conditions as follows.

To eliminate the secular term, it is necessary to first consider Eq. (2b), the third term of which becomes unbound with time. Thus, to ensure that the chase spacecraft does not drift away from the target spacecraft, the condition $\dot{y}_0 + 2nx_0 = 0$ must be used.

Using the above constraint, for some initial *x*-axis displacement, the motion of the chase spacecraft will describe an ellipse in the *x*-*y* plane with a major- to minor-axis ratio of 2:1 (the major axis being along the *y*-axis). This can be shown analytically, since when $\dot{y}_0 + 2nx_0 = 0$ the final term of Eq. (2a) becomes zero, and with $\dot{x}_0 = y_0 = 0$ the final term of Eq. (2b) also becomes zero, so that only the periodic terms of the two equations remain. The coefficients of the *y*-axis periodic terms are twice those of the *x*-axis terms, so the result is that the *y*-axis motion has an amplitude of oscillation which is twice that of the *x*-axis motion. An example of this bounded *x*-*y* plane motion is shown in Figure 2 for a target spacecraft in geostationary orbit.

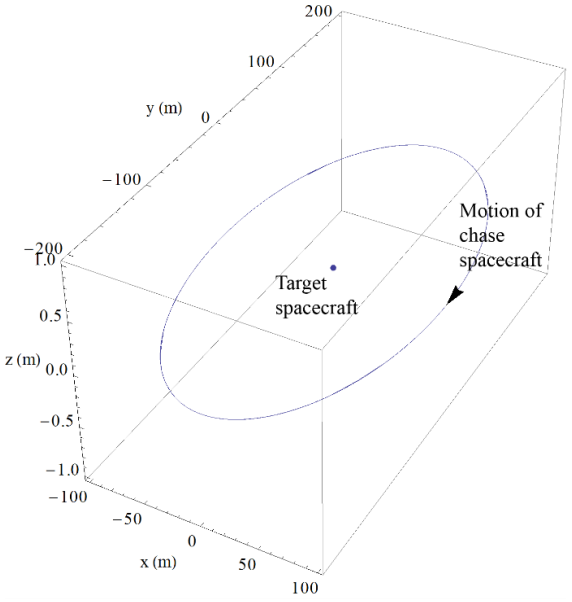

Figure 2. Bounded ballistic *x*-*y* plane motion with $\dot{y}_0 + 2nx_0 = 0$.

The above constraint allows multiple bound solutions to the classical Clohessy-Wiltshire equations, including the Projected Circular Orbit (PCO) [28] which causes the chase spacecraft to describe an apparent circle in the *y*-*z* plane, even though its three-dimensional motion is not truly circular. Recently, the feasibility of such orbits on a nanosatellite scale has been demonstrated by the University of Toronto Institute for Aerospace Studies (UTIAS) Canadian Advanced Nanospace Experiment (CanX) program, with the CanX-4 and CanX-5 spacecraft. Using carrier-phase differential GPS techniques for relative navigation, the two spacecraft successfully entered into along-track formations at ranges of 1000 m and 500 m, and PCO formations at 100m and 50m range [29].

By making a_x, a_y, and a_z nonzero, the classical solutions to the Clohessy-Wiltshire equations can now be augmented with the addition of continuous low thrust.

3. Static Formations

Continuous thrust can be used to generate locations at which a chase spacecraft may remain stationary with respect to the origin of a rotating frame. The simplest of low thrust augmented spacecraft formations, these artificial static equilibria are equivalent to the type III non-Keplerian orbits identified by McInnes [19].

Considering Eq. 1a-c, it is evident that for zero relative velocity between the chase and target spacecraft the required thrust-induced acceleration for all three axes must be

$$a_x = -3n^2 x \tag{4a}$$

$$a_y = 0 \tag{4b}$$

$$a_z = n^2 z \tag{4c}$$

It is clear, then, that static formations in which the chase spacecraft is displaced solely along the *y*-axis require zero thrust to maintain, and displacement along the *x*-axis requires three times the acceleration required for the same displacement along the *z*-axis. For a thrust vector $\boldsymbol{a} = [a_x, a_y, a_z]^{\mathrm{T}}$ of fixed magnitude, a surface can be plotted to illustrate all possible chase spacecraft positions for a range of *y* displacements. This plot is shown in Figure 3.

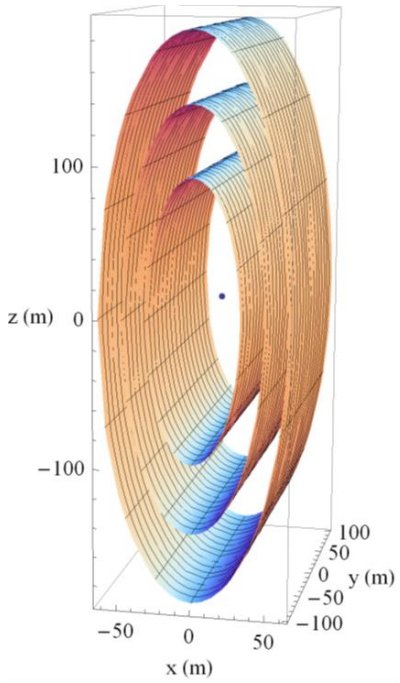

Figure 3. Surface plot of possible chase spacecraft positions for $-100\text{m} \leq y \leq 100\text{m}$, $|a| = 1 \times 10^{-6}$ ms^{-2}, 0.75×10^{-6} ms^{-2}, 0.5×10^{-6} ms^{-2}.

Perhaps a better understanding of the thrust requirements for such static formations can be gained from the vector field plot in Figure 4, where the required thrust vectors are shown across the *x*-*z* plane.

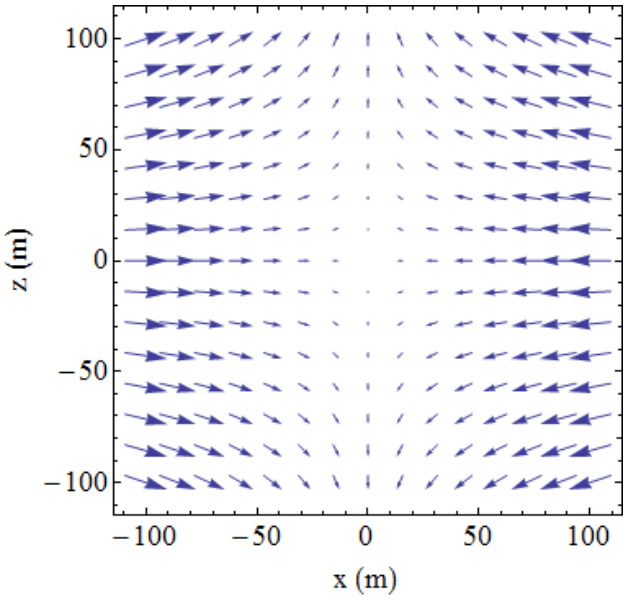

Figure 4. Required thrust vector field for static formation-flying in the *x*-*z* plane.

The Δv required to maintain a static position displaced in the *x*-direction, assuming independent thrusters aligned to each axis, since a_x is constant is

$$\Delta v_x = 3n^2 x\tau \quad (5)$$

where τ is the duration for which the formation is maintained. In a similar fashion, for a chase spacecraft position displaced in the *z*-direction, since a_z is also constant, the impulse required is found using

$$\Delta v_z = n^2 z\tau \quad (6)$$

Using these expressions, it can be shown that, in order to maintain a position displaced by 1 km in the *x*-axis for one year, the Δv required is approximately 503 ms^{-1}. Thus, assuming that the chase spacecraft is a microsatellite of initial mass 25 kg which uses axis-aligned micro ion thrusters with specific impulse of 3000 s, the mass of propellant required for one year is 0.424 kg. For a chase spacecraft displaced by 1 km along the *z*-axis, the Δv for one year is approximately 168 ms^{-1}, resulting in a propellant expenditure of only 0.142 kg. The thrust-induced acceleration magnitude required is very small (1.6×10^{-5} ms^{-2} for the *x*-displaced case).

These simple static formations have utility, however more interesting and varied new families of dynamic formations will now be explored.

4. Dynamic Formations

The bounded ballistic motion described in section 2 can be combined with or modified by continuous thrust to generate rich new families of relative orbits. In these cases, the chase spacecraft generally has nonzero relative velocity with respect to the target spacecraft (with instantaneous exceptions due to periodic oscillatory motion), and uses thrust in all three axes to produce potentially useful and interesting dynamic spacecraft formations.

4.1. Forced Circular Relative Orbits

A limitation of the unforced, free-flying bounded ballistic motion is that the chase spacecraft will always describe an ellipse about the target in the *x*-*y* plane. The maximum along-track displacement of the chase spacecraft will always be twice that of the radial displacement. Circular motion is not achievable in the ballistic case – the Projected Circular Orbit described in section 2 only appears to produce circular motion to an observer positioned radially below the spacecraft formation, and the *x*-*y* planar motion remains elliptical. However, it will now be shown that low thrust can be used to force the chase spacecraft to follow a circular relative orbit about the target in the rotating frame.

Interestingly, a simple forced circular relative orbit can be produced in the *x*-*y* plane with the application of thrust in only a single axis. Examining Eq. 1a and 1b, it is evident that the first term of Eq. 1a can be cancelled by selecting

$$a_x = -3n^2 x \quad (7)$$

so that the in-plane equations of motion now have the same amplitude and natural frequency: i.e. $\ddot{x} = 2n\dot{y}$ and $\ddot{y} = -2n\dot{x}$, when $a_y = 0$. In contrast to Figure 2, the resulting *x*-*y* plane circular motion is shown in Figure 5 for a target spacecraft in geostationary orbit with an initial displacement of $y_0 = 100$ m and initial velocity of $\dot{y}_0 = -2nx_0$, where all other initial conditions are zero.

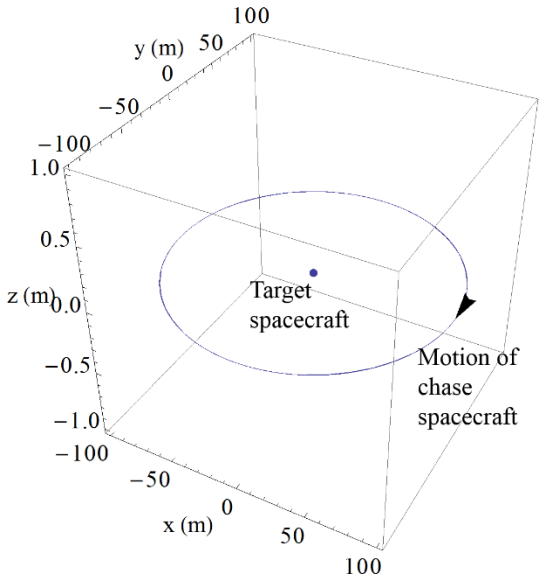

Figure 5. Forced circular relative orbit using single-axis thrust.

However, this approach only produces circular relative orbits in a single plane, and so a more general solution is now sought which permits a circle of any orientation about the target spacecraft.

It is possible to modify the shape and period of the *x*-, *y*-, and *z*-axis motion of the chase spacecraft so that it follows a circular relative trajectory about the target spacecraft, in any orientation. The angular velocity and radial distance between the target and chase spacecraft must be constant in the rotating frame, in this case.

To produce a circular trajectory about the target spacecraft, consider first the three-dimensional parametric equations of a circle

$$x(\theta) = c_1 + r\cos(\theta)\,\alpha_1 + r\sin(\theta)\beta_1 \tag{8a}$$

$$y(\theta) = c_2 + r\cos(\theta)\,\alpha_2 + r\sin(\theta)\beta_2 \tag{8b}$$

$$z(\theta) = c_3 + r\cos(\theta)\,\alpha_3 + r\sin(\theta)\beta_3 \tag{8c}$$

in which the vector $\boldsymbol{\alpha} = [\alpha_1, \alpha_2, \alpha_3]^T$ is collinear with the circle's transformed *x*-axis (transformed from the *x*-axis of the rotating frame, and fixed with respect to the circle), and the vector $\boldsymbol{\beta} = [\beta_1, \beta_2, \beta_3]^T$ is collinear with the transformed *y*-axis of the circle. Both $\boldsymbol{\alpha}$ and $\boldsymbol{\beta}$ are unit vectors. The circle's centre is $\boldsymbol{c} = [c_1, c_2, c_3]^T$, r is the radius of the circle, and θ is the angle between the radius vector and the *x*-axis measured in the anticlockwise direction about the circle's central axis. It is taken that $\theta = -\gamma nt$ (negative because the motion of the chase spacecraft in the *x*-*y* plane is clockwise), where γ is the ratio of the target spacecraft's Keplerian orbit period to the period of the circular relative orbit in the rotating frame (if $\gamma = 1$, then the period of the circular motion is equal to that of the Keplerian orbit of the target spacecraft), and where n and t have their usual meaning. The inclusion of γ also permits the modification of the period of the relative orbit.

Taking the first and second time derivatives of *x*, *y*, and *z* in Eq. 8a-c allows direct substitution into the augmented Clohessy-Wiltshire equations of Eq. 1a-c. It is then possible to obtain the required thrust-induced accelerations such that

$$a_x = n^2\big(-\mathrm{r}(\alpha_1(\gamma^2+3) - 2\beta_2\gamma)\cos(\gamma nt) + \mathrm{r}\big(2\alpha_2\gamma + \beta_1(\gamma^2+3)\big)\sin(\gamma nt) - 3c_1\big) \quad (9a)$$

$$a_y = -n^2 r\gamma((2\alpha_1 - \beta_2\gamma)\sin(\gamma nt) + (\alpha_2\gamma + 2\beta_1)\cos(\gamma nt)) \quad (9b)$$

$$a_z = n^2(-\alpha_3 r(\gamma^2 - 1)\cos(\gamma nt) + \beta_3 r(\gamma^2 - 1)\sin(\gamma nt) + c_3) \quad (9c)$$

The above general-case thrust commands can be used to produce a circular relative orbit with any orientation or angular velocity. A novel application for these equations will be described later in section 4.3, when they are combined with modified out-of-plane periodic motion.

4.2. Modified Out-of-Plane Motion

Examination of the Clohessy-Wiltshire equations of Eq. 1a-c shows that the *z*-axis motion is decoupled from the motion in the *x*-*y* plane. Using low thrust, the period of the natural oscillatory out-of-plane motion can be modified without affecting the motion in the other two axes: indeed, this augmented *z*-axis motion can be readily combined with other types of motion to produce interesting new relative trajectories.

In this case, in a fashion similar to the *z*-displaced artificial static equilibria, the *z*-axis thrust is made proportional to the *z*-axis displacement such that

$$a_z = \lambda^2 z \quad (10)$$

where

$$\lambda = n\sqrt{1 - \left(\frac{1}{k^2}\right)} \tag{11}$$

In which k can be considered the augmented period coefficient, so that the period of the z-direction motion is $T_z = kT$. Substituting Eq. 10 into Eq. 1c yields the new equation of out-of-plane motion

$$\ddot{z} = -\frac{n^2 z}{k^2} \tag{12}$$

which is a harmonic oscillator whose frequency can now be selected through the coefficient of the out-of-plane thrust law.

An example of this augmented out-of-plane motion, combined with bounded ballistic x-y plane motion, is shown in Figure 6 for a target spacecraft in geostationary orbit, where $k = 3$, $x_0 = z_0 = 100$ m, $y_0 = 0$, $\dot{x}_0 = \dot{z}_0 = 0$, and $\dot{y}_0 = -2nx_0$, propagated for three orbit periods.

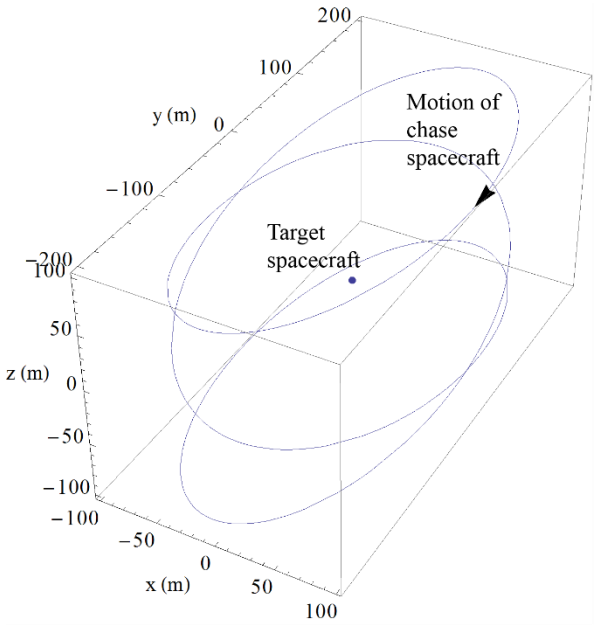

Figure 6. Relative motion of chase spacecraft with thrust proportional to z-axis displacement, k = 3.

The ability to modify the frequency of the oscillation along the z-axis independently of the motion in the other two axes finds application in the next section.

4.3. Sun Vector Tracking Orbit

A novel application of the two previously discussed families of forced dynamic formations is proposed whereby the chase spacecraft is caused to follow the Sun vector as it rotates about a

target in geostationary Earth orbit, in the rotating frame. The concept is described, in the Earth-centred inertial frame, in Figure 7 and Figure 8. Note that, in Figure 7, the Sun vector's relative motion around the target spacecraft will describe a circle in the orbit plane. Note also that, in Figure 8, the out-of-plane position of the chase spacecraft will have to oscillate with a period of one year. If it is assumed that the Earth has a circular orbit around the Sun, then the maximum and minimum Sun declinations will be equal and opposite so that the *z*-axis motion will be sinusoidal over time. Thus, the Sun vector tracking orbit requires that the in-plane and out-of-plane motion have periods of one solar day and one year respectively.

To generate the thrust commands for this kind of relative orbit, we first use the general-case forced circular relative orbit commands and simplify them since the circular relative orbit is in the *x*-*y* plane. Since the two unit vectors, $\boldsymbol{\alpha}$ and $\boldsymbol{\beta}$, are $[1, 0,0]^T$ and $[0,1,0]^T$ respectively, and the *x* and *y* locations of the circle centre are $c_1 = c_2 = 0$, Eq. 9a and 9b simplify to

$$a_x = -n^2 r(\gamma^2 - 2\gamma + 3)\cos(\gamma n t) \tag{13a}$$

$$a_y = -n^2 r\gamma(2 - \gamma)\sin(\gamma n t) \tag{13b}$$

For the *z*-axis cycle, we use $a_z = \lambda^2 z$, where $\lambda = n\sqrt{1 - \left(\frac{1}{k^2}\right)}$ as in Eq. 10 and Eq. 11, respectively. The two constants *k* and γ are selected as 365.25 (the number of days in the Julian year) and 0.99727 (the ratio of sidereal day to solar day), respectively.

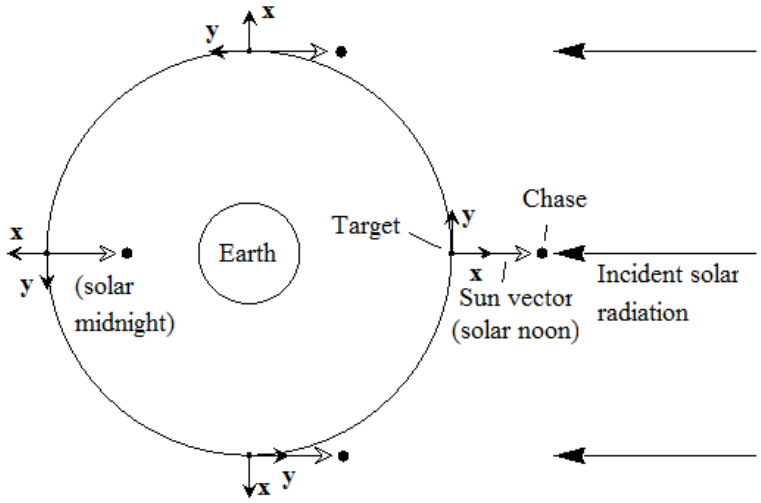

Figure 7. Sun vector tracking in GEO, viewed from the direction of the Earth's spin axis.

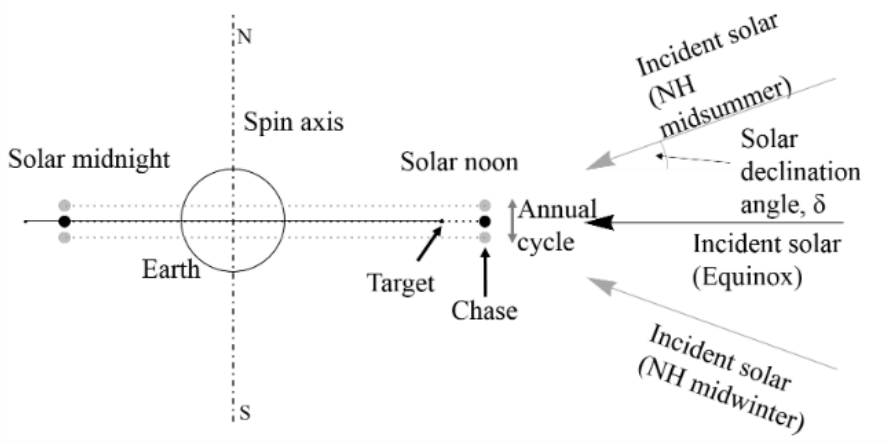

Figure 8. Sun vector tracking in GEO, viewed from equatorial plane.

When these thrust commands are used, for a chase spacecraft beginning its orbit at local solar noon at the minimum annual Sun declination angle, the resulting motion is shown in Figure 9.

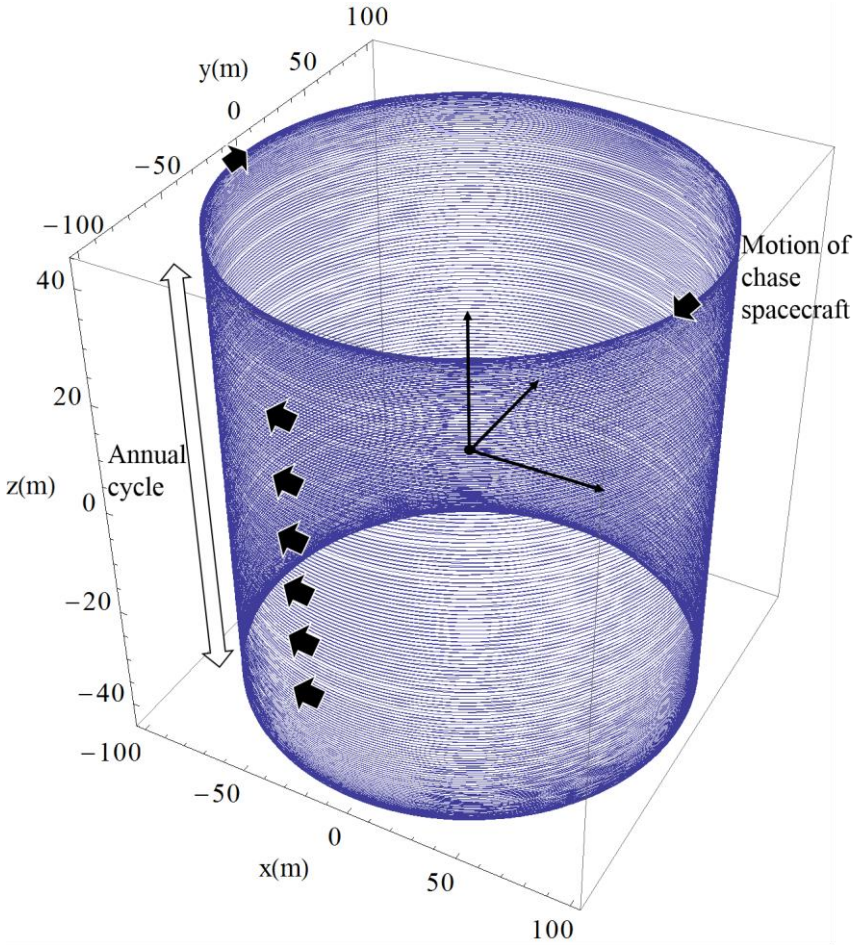

Figure 9. Relative trajectory of chase spacecraft tracking the Sun vector about the target spacecraft for one year.

The impulse requirements for this type of orbit are found by integrating the thrust-induced acceleration in each axis (assuming independent body-mounted thrusters) as piecewise functions since the thrust changes direction with each plane crossing. For a Sun vector tracking relative orbit with in-plane radius of 100 m and out-of-plane displacement range of ± 43.3 m, then the total Δv for maintaining the orbit for one year is 36.66 ms^{-1}.

5. Orbit Transfers in the Rotating Frame

An interesting solution to patching between non-Keplerian and Keplerian orbits in the rotating frame is presented. Since the non-Keplerian orbit requires continuous low thrust to be maintained, it is considered operationally advantageous to design a transfer manoeuvre which can be accomplished by using either zero thrust or only low thrust. As such, the first manoeuvre presented is the ballistic transfer, which requires zero thrust.

Assuming the chase spacecraft is in a non-Keplerian orbit (with initial out-of-plane displacement z_0, such that $a_z = n^2 z_0$) with bounded in-plane motion (as described in section 2, with $\dot{y}_0 + 2nx_0 = 0$), then to transfer to an oppositely-displaced non-Keplerian orbit with displacement $-z_0$ it is necessary only to disable the thrust. The chase spacecraft will, over one half of an orbit period, follow a ballistic arc until it reaches $-z_0$, at which point the thrust is resumed with $a_z = -n^2 z_0$. Clearly, this type of manoeuvre requires zero impulse and therefore zero propellant to perform, with its primary disadvantage being that it will always require one half of an orbit period to complete. The relative trajectory of the chase spacecraft while performing this manoeuvre between two symmetrically displaced non-Keplerian orbits is displayed in Figure 10, for $z_0 = 100$ m.

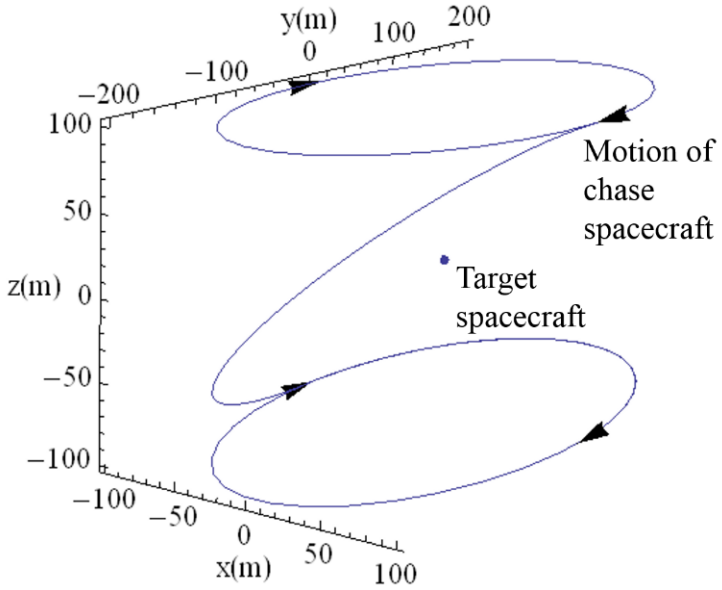

Figure 10. Ballistic patching between displaced NKOs in the rotating frame.

Alternatively, if a shorter transfer time or flatter trajectory is desirable, low thrust can be used to achieve the transfer by modifying the out-of-plane period as described in section 4.2 (so that $a_z = \lambda^2 z$). In this case, to perform the transfer in less than one orbit period, the augmented period coefficient k must be selected as $k < 1$ for the duration of the transfer. The disadvantage of this method is that the peak thrust required to perform the transfer is greater than that required to

maintain the NKO, and so the suitability of this manoeuvre type depends on the capabilities of the selected propulsion technology. The relative trajectory of the chase spacecraft in the rotating frame is shown in Figure 11, where $z_0 = 100$ m and $k = 0.5$, and the orbit transfer duration is 0.25 orbit periods. In this case, the peak thrust induced acceleration magnitude required for the manoeuvre is approximately 1.6×10^{-6} ms^{-2}, which is three times that required to simply maintain the NKO.

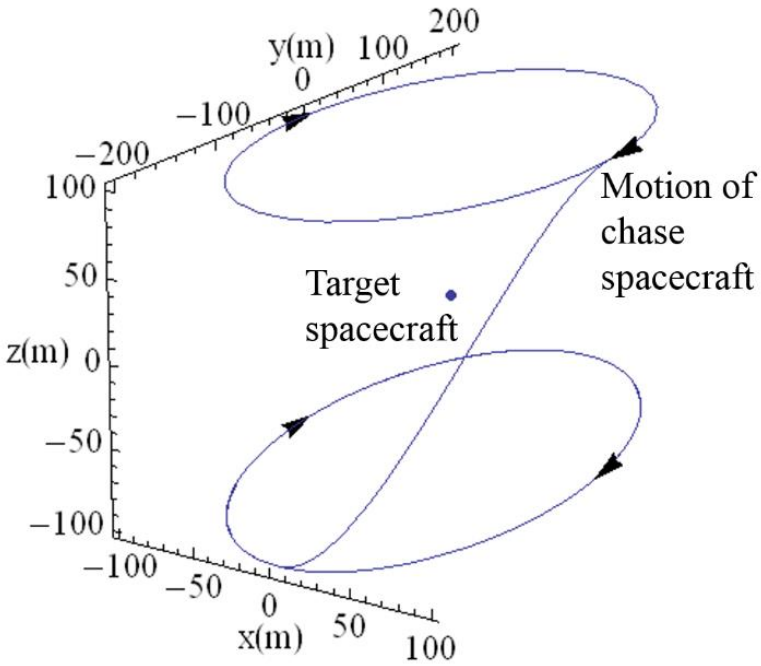

Figure 11. Forced low-thrust patching between displaced NKOs in the rotating frame (*k* = 0.5).

6. Summary and Conclusions

In this study, rich new families of relative orbits have been analytically described and explored, for a two-spacecraft formation in Earth orbit. It has been shown that continuous low thrust can be used to augment spacecraft formations by permitting relative flight on forced Keplerian and non-Keplerian trajectories. For relatively small impulse and therefore small propellant expenditure, statically displaced formations and modified-period relative orbits can be generated. This work presents three primary advances, namely the generic thrust commands for the creation of forced circular relative orbits in the rotating frame with arbitrary period and orientation, the analytical description of a forced relative orbit in which one spacecraft tracks the Sun vector around a target spacecraft in a circular Earth orbit, and a novel approach for transferring between displaced non-Keplerian and Keplerian orbits in the rotating frame using either propellantless ballistic manoeuvres or out-of-plane low thrust alone.

7. Acknowledgements

The authors would like to thank Dr. Robert McKay, Dr. Malcolm Macdonald, and Dr. James Biggs of the University of Strathclyde for their contributions to this research. This research was funded by the Engineering and Physical Sciences Research Council (EPSRC) Doctoral Training Grant.

8. References

[1] Alfriend, K. T., Vadali, S. R., Gurfil, P., How, J. P., Breger, L. S., "Introduction," *Spacecraft Formation Flying: Dynamics, Control and Navigation*, 1st ed., Elsevier, Oxford, 2009, pp. 1-11.

[2] Sholomitsky, G. B., Prilutsky, O. F., Rodin, V. G., "Infra-red space interferometer," *28th International Astronautical Federation Congress*, Prague, Czechoslovakia, IAF-77-68, 1977.

[3] Labeyrie, A., "Stellar interferometry methods," *Annual Review of Astronomy and Astrophysics*, Vol. 16, No. 1, 1978, pp. 77-102.

[4] Llorente, J. S., Agenjo, A., Carrascosa, C., De Negueruela, C., Mestreau-Garreau, A., Cropp, A., Santovincenzo, A., "PROBA-3: precise formation flying demonstration mission," *Acta Astronautica*, Vol. 82, No. 1, 2013, pp. 38-46.

doi: 10.1016/j.actaastro.2012.05.029

[5] Anaro-Seoane, P., Aoudia, S., Babak, S., Binétruy, P.,Berti, E., Bohé, A., Caprini, C., Colip, M., Cornish, N. J., Danzmann, K., Dufaux, J.-F., Gair, J., Jennrich, O., Jetzer, P., Klein, A., Lang, R. N., Lobo, A., Littenberg, T., McWilliams, S. T., Nelemans, G., Petiteau, A., Porter, E. K., Schutz, B. F., Sesana, A., Stebbins, R., Sumner, T., Vallisneri, M., Vitale, S., Volonteri, M., Ward, H., "e-LISA: astrophysics and cosmology in the millihertz regime," *GW Notes*, Vol. 6, 2012, pp. 4-110.

[6] Jacobovits, A., Vaneck, T. W., "AeroAstro's Escort – a microsatellite for on-orbit inspection of space assets," *17th Annual AIAA/USU Conference on Small Satellites*, SSC03-IV-7, 2003.

[7] Scharf, D. P., Hadaegh, F. Y., Ploen, S. R., "A survey of spacecraft formation flying guidance and control (part I): guidance," *Proceedings of the 2003 American Control Conference*, Vol. 2, Denver, Colorado, 2003, pp. 1733-1739.

doi: 10.1109/ACC.2003.1239845

[8] Scharf, D. P., Hadaegh, F. Y., Ploen, S. R., "A survey of spacecraft formation flying guidance and control (part II): control," *Proceedings of the 2004 American Control Conference*, Vol. 4, Boston, Massachusetts, 2004, pp. 2976-2985.

[9] Austin, R. E., Dod, R. E., Terwilliger, C. H., "The ubiquitous solar electric propulsion stage," *Acta Astronautica*, Vol. 4, No. 5-6, 1977, pp. 671-694.

[10] Natarajan, A., Schaub, H., "Linear dynamics and stability analysis of a two-craft Coulomb tether formation," *Journal of Guidance, Control, and Dynamics*, Vol. 29, No. 4, 2006, pp. 831-839.

doi: 10.2514/1.16480

[11] Schaub, H., Hussein, I. I., "Stability and reconfiguration analysis of a circularly spinning two-craft Coulomb tether," *IEEE Transactions on Aerospace and Electronic Systems*, Vol. 46, No. 4, 2010, pp. 1675-1686.

doi: 10.1109/AERO.2007.352670

[12] Cen, J. W., Xu, J. L., "Performance evaluation and flow visualization of a MEMS based vaporizing liquid micro-thruster," *Acta Astronautica*, Vol. 67, No. 3-4, 2010, pp. 468-482.

[13] Wirz, R., Gale, M., Mueller, J., Marrese, C., "Miniature ion thrusters for precision formation flying," *40th AIAA/ASME/SAE/ASEE Joint Propulsion Conference and Exhibit*, Fort Lauderdale, Florida, AIAA 2004-4115, 2004.

doi: 10.2514/6.2004-4115

[14] Dusek, H. M., "Motion in the vicinity of libration points of a generalized restricted three-body model," *Progress in Astronautics and Aeronautics*, Vol. 17, 1966, pp. 37-54.

[15] Nock, K. T., "Rendezvous with Saturn's rings," *Planetary rings: 1st international meeting*, CNES, Toulouse, France, 1984, pp. 743-759.

[16] Yashko, G. J., Hastings, D. E., "Analysis of thruster requirements and capabilities for local satellite clusters," *10th AIAA/USU Conference on Small Satellites*, AIAA, Logan, Utah, 1996.

[17] Baig, S., McInnes, C. R., "Artificial three-body equilibria for hybrid low-thrust propulsion," *Journal of Guidance, Control, and Dynamics*, Vol. 31, No. 2, 2008, pp. 1644-1655.

doi: 10.2514/1.36125

[18] Heiligers, J., McInnes, C. R., Biggs, J. D., Ceriotti, M., "Displaced geostationary orbits using hybrid low-thrust propulsion," *Acta Astronautica*, Vol. 71, 2012, pp. 51-67.

doi: 10.1016/j.actaastro.2011.08.012

[19] McInnes, C. R., "The existence and stability of families of displaced two-body orbits," *Celestial Mechanics and Dynamical Astronomy*, Vol. 67, No. 2, 1997, pp. 167-180.

doi: 10.1023/A:1008280609889

[20] McInnes, C. R., "Dynamics, stability, and control of displaced non-Keplerian orbits," *Journal of Guidance, Control, and Dynamics*, Vol. 21, No. 5, 1998, pp. 799-805.

doi: 10.2514/2.4309

[21] Scheeres, D. J., "Stability of hovering orbits around small bodies," *Advances in the Astronautical Sciences*, Vol. 102, 1999, pp. 855-875.

[22] Xu, M., Xu, S., "Nonlinear dynamical analysis for displaced orbits above a planet," *Celestrial Mechanics and Dynamical Astronomy*, Vol. 102, No. 4, pp. 327-353, 2008.

doi: 10.1007/s10569-008-9171-4

[23] Bombardelli, C., Peláez, J., "On the stability of artificial equilibrium points in the circular restricted three-body problem," *Celestial Mechanics and Dynamical Astronomy*, Vol. 109, No. 1, 2011, pp. 13-26.

doi: 10.1007/s10569-010-9317-z

[24] Ceriotti, M., McInnes, C. R., "Natural and sail-displaced doubly-symmetric Lagrange point orbits for polar coverage," *Celestial Mechanics and Dynamical Astronomy*, Vol. 114, No. 1-2, 2012, pp. 151-180.

doi: 10.1007/s10569-012-9422-2

[25] Aliasi, G., Mengali, G., Quarta, A. A., "Artificial equilibrium points for a generalized sail in the elliptic restricted three-body problem," *Celestial Mechanics and Dynamical Astronomy*, Vol. 114, No. 1-2, 2012, pp. 181-200.

doi: 10.1007/s10569-012-9425-z

[26] McKay, R. J., Macdonald, M., Biggs, J., McInnes, C. R., "Survey of highly non-Keplerian orbits with low-thrust propulsion," *Journal of Guidance, Control, and Dynamics*, Vol. 34, No. 3, 2011, pp. 645-666.
doi: 10.2514/1.52133

[27] Wiltshire, R. S., Clohessy, W. H., "Terminal guidance system for satellite rendezvous," *Journal of the Aerospace Sciences*, Vol. 27, No. 9, 1960, pp. 653-658.

[28] Vaddi, V., "Modelling and control of satellite formations," PhD thesis, Texas A and M University, 2003.

[29] Orr, N. G., Eyer, J. K., Larouche, B. P., Zee, R. E., "Precision formation flight: the CanX-4 and CanX-5 dual nanosatellite mission," *21st Annual AIAA/USU Conference on Small Satellites*, SSC07-VI-2, 2007.